This article has been accepted for publication in IEEE Transactions on Vehicular Technology. This is the author's version which has not been fully edited and content may change prior to final publication. Citation information: DOI 10.1109/TVT.2026.3661626

RIS-Assisted Joint Transmitter-Receiver Space Shift Keying Design for Highly Flexible Wireless Communications

Ming Yue, Yuyang Peng, *Senior Member, IEEE*, Runlong Ye, Juho Lee, *Fellow, IEEE*, Fawaz Al-Hazemi, *Senior Member, IEEE*, and Raouf Boutaba, *Fellow, IEEE*

***Abstract*—This paper presents a novel scheme for Reconfigurable Intelligent Surface assisted Joint Transmitter-Receiver Space Shift Keying (RIS-JTRSSK), which achieves a higher Spectral Efficiency (SE) and a more flexible transmission. In the proposed scheme, the incoming bits are divided into three groups, where the first group is used to determine the number of active antennas in the transmitter and the receiver, and the remaining two groups are used to respectively determine the transmit and receive antennas combinations. Moreover, we study the transmission design of RIS-JTRSSK scheme in both cases of perfect and imperfect channel state information. The theoretical Bit Error Rate (BER) of RIS-JTRSSK is also investigated and an antenna selection algorithm as well as a fast elimination algorithm are proposed to further improve the BER performance of RIS-JTRSSK and reduce complexity, respectively. Meanwhile, a low-complexity detector is designed as an alternative method to maximum likelihood detector for reducing detection complexity along with complexity analysis. Finally, RIS assisted flexible transmitter-receiver space shift keying scheme is proposed as flexible version that enables a richer set of application scenarios. We evaluate the BER performance of RIS-JTRSSK and compare it with that of large intelligent surface assisted spatial modulation. In addition, two benchmark schemes, namely Intelligent Reflecting Surface (IRS) assisted transceiver space shift keying and IRS assisted transceiver generalized space shift keying are used to demonstrate the system performance of our proposed scheme. The simulation results prove that our proposed schemes has good BER performance and can achieve higher SE with the same number of antennas.**

***Index Terms*—Reconfigurable intelligent surface, joint space shift keying, antenna selection, fast elimination, spectral efficient transmission, complexity.**

I. Introduction

WHILE the massive Multiple-Input Multiple-Output (MIMO) and millimeter-wave technologies pivotal to fifth-generation (5G) networks have ushered in unprecedented data rates, they often come at the cost of high energy consumption and complex hardware. Index Modulation (IM) emerges as a promising physical-layer paradigm to mitigate these challenges [1], [2]. By encoding additional information into the indices of transmission entities, i.e. active antennas or frequency subcarriers, IM achieves compelling trade-offs among Spectral Efficiency (SE), energy efficiency, and hardware simplicity. Notable implementations like Spatial Modulation (SM) [3] and Space Shift Keying (SSK) [4] exemplify this principle by leveraging antenna indices for information conveyance, establishing a foundation for energy-efficient spectral enhancement.

Looking toward the sixth-generation (6G) era, wireless systems must support a confluence of drastically higher throughput, ultra-low latency, and massive connectivity for Internet-of-Things (IoT) applications, which objectives that stretch beyond current 5G capabilities [5], [6]. This demands innovative communication frameworks, among which Reconfigurable Intelligent Surface (RIS)-assisted transmission has gained considerable attraction [7], [8]. An RIS comprises an array of nearly passive and low-cost elements that dynamically manipulate electromagnetic waves via a software-defined controller. Unlike active antenna arrays, RIS operates without power-hungry radio-frequency (RF) chains, acting as an energy-efficient passive beamformer that can significantly enhance coverage and link strength [9]–[12]. Its unique ability to smartly reconfigure wireless environments positions RIS as a key enabler for future 6G networks.

To harness the complementary benefits of RIS and IM, recent studies have explored their integration to enhance system performance. Initial work in [13] introduced IM into RIS-aided systems by employing SM/SSK at the receiver, demonstrating significant Bit Error Rate (BER) improvement. Subsequent research proposed two full-duplex schemes using RIS for energy-efficient and robust transmission [14], [15]. In [16], a Multiple-Input Single-Output (MISO) framework was used to study RIS-assisted transmitted SSK, where information is encoded in transmit antenna indices, mitigating synchronization and interference issues. Inspired by [16], a new RIS-assisted transmitted SSK was proposed in [17] to enhance the SE by utilizing the number of activated antennas to transmit additional bits. Another RIS-assisted SSK scheme was proposed in [18], which realizes passive beamforming by optimizing the reflection phases, and the RIS can transmit its own Alamouti-coded information while reflecting SSK signals to the receiver. Meanwhile, based on Single-Input Multiple-Output (SIMO) model, an RIS-assisted receive generalized

This work was supported by the Science and Technology Development Fund, Macau SAR (0085/2024/RIA2).

Ming Yue, Yuyang Peng, and Runlong Ye are with School of Computer Science and Engineering, Macau University of Science and Technology, Macau, China (e-mail: 3230002258@student.must.edu.mo; 3220002479@student.must.edu.mo; yypeng@must.edu.mo). (*Corresponding author: Yuyang Peng*.)

Juho Lee is with Samsung Research, Samsung Electronics, Seoul, Korea (e-mail: Juho95.lee@samsung.com).

Fawaz Al-Hazemi is with the Department of Computer and Network Engineering, University of Jeddah, Jeddah 21959, Saudi Arabia (e-mail: fmalhazemi@uj.edu.sa).

Raouf Boutaba is with the David R. Cheriton School of Computer Science, University of Waterloo, Waterloo, ON N2L 3G1, Canada (e-mail: rboutaba@uwaterloo.ca).

Authorized licensed use limited to: University of Waterloo. Downloaded on March 25,2026 at 00:16:41 UTC from IEEE Xplore. Restrictions apply.
© 2026 IEEE. All rights reserved, including rights for text and data mining and training of artificial intelligence and similar technologies. Personal use is permitted, but republication/redistribution requires IEEE permission. See https://www.ieee.org/publications/rights/index.html for more information.

This article has been accepted for publication in IEEE Transactions on Vehicular Technology. This is the author's version which has not been fully edited and content may change prior to final publication. Citation information: DOI 10.1109/TVT.2026.3661626

SSK (GSSK) scheme was proposed in [19]. In this approach, the authors used the receive antennas combinations to convey information, this way using fewer antennas to achieve the same SE. In addition, in order to obtain higher data rate, researchers have begun to extend SSK into SM domain. In [20], a high SE scheme named RIS assisted extended variable SM was proposed, where the authors used the different transmission modes to determine the number of active antennas where each transmission mode has its own symbol modulation order. Meanwhile, an RIS-aided transmit SM system for downlink transmission was proposed in [21], which introduced three distinct detectors at the receiver for signal recovery. Subsequently, an RIS-aided flexible receive SM scheme that adaptively selects the number of active antennas, and a power-sensing RIS-aided SM scheme were proposed in [22] and [23], respectively. The former provides enhanced system flexibility while maintaining SE, whereas the latter addresses the limitation on SE without compromising BER performance.

In the above mentioned schemes, as RIS-assisted IM schemes typically improve SE through enhancing antenna numbers or modulated symbols, this inevitably increases system complexity. Consequently, researchers have focused on the development of high SE transmission schemes from a different perspective. In [24], the authors applied forth quadrature SSK scheme assisted by RIS to augment SE by decomposing the spatial domain. In this work, a max-min optimization is performed to maximize the received Signal-to-Noise Ratio (SNR) components of the two chosen receiving antennas. Subsequently, a new RIS-assisted quadrature SM scheme was proposed in [25], which uses a novel method to adjust the phase shifts of the RIS elements to maximize the SNR. In [26], the authors proposed a novel uplink mmWave communication system that utilizes spatial scattering modulation to further improve the SE. Another prevalent approach involves creating distinct reflection patterns by regulating the ON/OFF conditions of the RIS reflection elements, enabling it to convey extra information [27], [28]. Subsequently, a Reflection Pattern Modulation (RPM) communication system was introduced in [29], which partitions the RIS to enhance the MISO system. Concurrently, a combined active and passive beamforming approach was proposed in [30] where the authors combined RPM with GSSK modulation and put forward a new RIS-assisted GSSK scheme for achieving high SE transmission by using reflection patterns. Additionally, a novel phase configuration scheme for RIS-assisted SSK signaling with passive beamforming was proposed in [31]. This scheme allows the phases to be adjusted at a relatively low rate, which is no less than the reciprocal of the channel coherence time, thereby substantially reducing system overhead and enhancing SE. However, the shortcomings of these approaches stem from the underexploitation of RIS potential and the intricate optimization challenge. To alleviate these shortcomings and improve SE, some research works extended the IM technology to both transmitter and receiver as an alternative approach. In [32], based on MIMO model, a practical frame of LIS-assisted SM (RIS-SM) scheme was proposed, which utilizes both transmit and receive antenna indices as well as symbol modulation orders to enhance the SE. In addition, an RIS-assisted joint transceiver SSK reflection modulation scheme was proposed in [33]. In this scheme, the RIS-assisted transceiver performs SSK modulation and simultaneously inserts extra bits into the reflected phase shift of the RF signal.

A. Motivations and Contributions

It is evident from the aforementioned studies that utilizing reflection pattern for index inevitably compromises the performance of RIS and it can bring difficult optimization problems, while only using transceiver antennas or symbol modulation orders to achieve high SE will increase the complexity of the system. Furthermore, these schemes lack flexibility and have limited applicability. Specifically, the underlying system models are fixed and cannot be flexibly adjusted to accommodate different application scenarios or requirements. This paper introduces a novel RIS-assisted IM scheme that achieves higher SE and flexibility, which can be considered as a generalization of RIS-assisted SSK modulation. The main contributions of this work can be summarized as follows

- We propose an RIS-assisted Joint Transmitter-Receiver Space Shift Keying (RIS-JTRSSK) scheme, wherein the number of active antennas at both the transmitter and receiver are controlled using extra bits. Specifically, the transceiver adopts different modulation techniques including SSK modulation or GSSK modulation. This approach enhances SE and flexibility compared to the conventional RIS-assisted IM scheme without significant additional complexity or cost. Furthermore, we also derive a closed-form theoretical BER of the RIS-JTRSSK scheme.
- Given the practical difficulty of obtaining perfect Channel State Information (CSI), we discuss the transmission design of the RIS-JTRSSK scheme in two cases: Perfect CSI and imperfect CSI. Specifically, drawing on the findings from [34], we put forward two bounded CSI error models: Imperfect RIS-Receiver Channels (IRRC) and Imperfect Cascaded Transmitter-RIS-Receiver Channels (ICTRRC).
- To further bolster the system's flexibility and SE, a versatile variant of RIS-JTRSSK named RIS-assisted Flexible Transmitter-Receiver Space Shift Keying (RIS-FTRSSK) scheme is proposed. Specifically, we modify the bit mapping mechanism of RIS-JTRSSK scheme so that the number of active antennas at the transmitter and at the receiver are determined by different groups of bits. This way, these two schemes, along with RIS-JTRSSK, can support more user application scenarios
- Based on the findings in [32], [35], [36], the RIS-JTRSSK with antenna selection is introduced to attain superior BER performance. Furthermore, a Fast Elimination Algorithm (FEA) is introduced for antenna selection, aiming to minimize complexity. Also, a Low-Complexity (LC) detector is proposed as an alternative to the Maximum Likelihood (ML) detector, with the goal of minimizing detection complexity.
- We evaluate BER performance of the RIS-JTRSSK system via simulations, by comparing with the RIS-SM

Authorized licensed use limited to: University of Waterloo. Downloaded on March 25,2026 at 00:16:41 UTC from IEEE Xplore. Restrictions apply.
© 2026 IEEE. All rights reserved, including rights for text and data mining and training of artificial intelligence and similar technologies. Personal use is permitted, but republication/redistribution requires IEEE permission. See https://www.ieee.org/publications/rights/index.html for more information.

This article has been accepted for publication in IEEE Transactions on Vehicular Technology. This is the author's version which has not been fully edited and content may change prior to final publication. Citation information: DOI 10.1109/TVT.2026.3661626

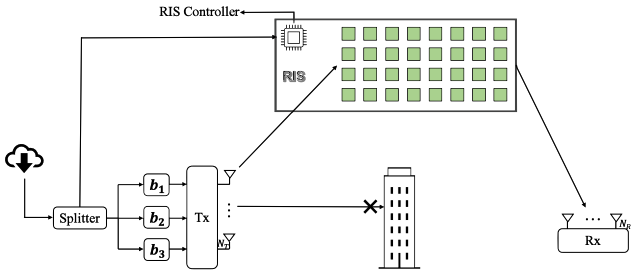

Fig. 1. System model of the proposed RIS-JTRSSK scheme.

scheme [32]. Additionally, we provide two benchmark schemes: RIS-assisted Transceiver SSK (RIS-TRSSK) and RIS-assisted Transceiver GSSK (RIS-TRGSSK) for more comprehensive experimental results. The results show that the RIS-JTRSSK system surpasses these contrastive schemes and achieves higher SE under the same system configuration.

B. Organization and Notations

Organization: The system model of the proposed RIS-JTRSSK scheme is introduced in Section II, while the closed-form of theoretical BER and the related analysis are presented in Section III. In Section IV, the system of RIS-FTRSSK is presented. The antenna selection method and FEA are described in Section V. Then, the LC detector and detection complexity analysis are provided in Section VI. Simulation results are presented in Section VII. Finally, conclusions are drawn in Section VIII.

Notations: Boldface lowcase and uppercase letters are used for column vectors and matrices, respectively. The real and imaginary parts of a complex variable are denoted by $\{\cdot\}_R$ and $\{\cdot\}_I$, respectively. $\mathcal{CN}(\mu, \sigma^2)$ stands for a complex Gaussian random variable (RV) with mean μ and variance σ^2. $M_X(\cdot)$ is the Moment Generating Function (MGF) of an RV and $Q(\cdot)$ stands for the Gaussian Q-function. The identity matrix is denoted by $\mathbf{I}$.

II. System Model

In this section, we present the system model for the proposed RIS-JTRSSK scheme as illustrated in Fig. 1. We also discuss the transmission design under perfect CSI and imperfect CSI, respectively. Specifically, we construct the proposed schemes by obstructing the direct link between the transmitter and receiver, as a shadow communication scenario. Therefore, the RIS is deployed in the system to assist the information transmission. It is exploited as a reflector in a dual-hop communication system between transmitter with N_T transmit antennas and receiver with N_R receive antennas. The RIS is equipped with N low-cost passive reflection elements and can adjust the phase of the incident wave using an RIS controller to maximize the SNR at the receiver.

A. Transmission Design with Perfect CSI

To achieve the theoretical passive beamforming gain offered by RIS-assisted systems, it is conventionally assumed that perfect CSI for all cascaded RIS-aided channels is available. To satisfy this requirement, some researches have designed channel acquisition methods for RIS-assisted systems. In single-user systems, researchers have proposed several compressive sensing based methods to develop various low pilot overhead channel estimation schemes [37]–[39]. While, for multi-user systems, since all users share the common base station-RIS channel, additional structural characteristics are exploited to enhance channel estimation precision when reducing the pilot overhead [40], [41]. As such, some of the channel estimation problems in RIS-assisted systems have been addressed. In this case, the wireless channel is assumed to be frequency flat with Rayleigh fading gains, and the CSI from the transmitter to the RIS and from the RIS to the receiver are assumed to be known in the RIS controller via a communication software, while the transmitter and the receiver can also obtain the perfect CSI. In RIS-JTRSSK system model, the incoming bits are divided into three parts, i.e., b_1, b_2 and b_3. The first b_1 bit part represents the number of antennas activated by the transmitter and receiver, which is denoted as J ($1 \leq J \leq \frac{N_L}{2}$). It is worth noting that $N_L = \min(N_T, N_R)$. In addition, in order to ensure the high SE and low system complexity, we set the range of active antennas as 1 to $\frac{N_L}{2}$[1]. In this way, the same number of antennas are activated by the transmitter and the receiver in each time slot. Therefore, in the RIS-JTRSSK system, the the transmitter and the receiver respectively adopt SSK modulation or GSSK modulation based on the first bit part in each time slot. After J is determined, the number of the transmit antenna combinations and receive antenna combinations can be calculated as $M_T = \binom{N_T}{J}$ and $M_R = \binom{N_R}{J}$, respectively. Additionally, the sets of transmit combinations and receive combinations based on J active antennas are denoted as $\mathcal{A}_T$ and $\mathcal{A}_R$, respectively. In this manner, S_T out of M_T transmit antenna combinations are selected from $\mathcal{A}_T$ to map b_2 bit part and S_R out of M_R receive antenna combinations are selected from $\mathcal{A}_R$ to map b_3 bit part[2]. Therefore, the SE can be calculated by:

$$r = \log_2(\frac{N_L}{2}) + \log_2(S_T) + \log_2(S_R), \tag{1}$$

TABLE I
Mapping For RIS-JTRSSK Scheme with $N_L = N_R = 4$

b_1	Active antenna	b_2	S_T	b_3	S_R
0	1	00	1-th	00	2-th
		01	6-th	01	3-th
		10	3-th	10	4-th
		11	7-th	11	1-th
1	2	00	(1,2)	00	(1,3)
		01	(2,8)	01	(1,4)
		10	(3,6)	10	(2,3)
		11	(4,7)	11	(2,4)

[1]The maximum number of active antennas can be adjusted according to different requirements. Specifically, the system's SE increases only when the number of active antennas is a power of two. Therefore, if the system complexity and BER performance are the priority metrics, we can set the maximum number of active antennas to $\frac{N_L}{4}$. In addition, if the SE is the priority metric, we can set the maximum number of active antennas to N_L.

[2]To maintain low system complexity and comparable BER performance, the maximum values of S_T and S_R cannot exceed the maximum number of transmit and receive antennas, respectively, and both must be power of two.

Authorized licensed use limited to: University of Waterloo. Downloaded on March 25,2026 at 00:16:41 UTC from IEEE Xplore. Restrictions apply.
© 2026 IEEE. All rights reserved, including rights for text and data mining and training of artificial intelligence and similar technologies. Personal use is permitted, but republication/redistribution requires IEEE permission. See https://www.ieee.org/publications/rights/index.html for more information.

This article has been accepted for publication in IEEE Transactions on Vehicular Technology. This is the author's version which has not been fully edited and content may change prior to final publication. Citation information: DOI 10.1109/TVT.2026.3661626

where the length of b_2 and b_3 are determined by $\log_2(S_T)$ and $\log_2(S_R)$, respectively[3]. Here is an example for RIS-JTRSSK scheme with $N_T = 8$ and $N_R = 4$.

Example: Firstly, according to $N_L = \min(N_T, N_R)$, we obtain $N_L = N_R = 4$. By assigning $S_T = 4$ and $S_R = 4$, the SE is calculated as 5 bits/s/Hz and the mapping table is presented in Table I. Suppose that the incoming bits are 10011, which are separated into three parts as $b_1 = 1$, $b_2 = 00$ and $b_3 = 11$. Referring to Table I, both the transmitter and receiver activate two antennas based on $b_1 = 1$, respectively. Taking $b_2 = 00$ and $b_3 = 11$ into account, the transmitter selects its first antenna combination (1,2) to transmit, while the receiver selects its fourth antenna combination (2,4) to receive signal. Consequently, the information bits 10011 are conveyed by RIS-JTRSSK scheme.

Based on the working principle of our propose scheme, the number of antennas activated by the receiver varies in different time slots. Therefore, the RIS is divided into J parts according to J number of active antennas in each time slot and each part has $\lfloor \frac{N}{J} \rfloor$ reflection elements. For simplicity, we assume that all channels in the proposed scheme follow Rayleigh distribution that $\mathcal{CN}(0,1)$ without loss of generality. The channel between the active transmit antennas and $(\lfloor \frac{N}{J} \rfloor (j-1)+d)$-th element of the RIS is:

$$\begin{aligned} &h_{\lfloor \frac{N}{J} \rfloor (j-1)+d,k_{(1)}} + \cdots + h_{\lfloor \frac{N}{J} \rfloor (j-1)+d,k_{(J)}} \\ =&\alpha_{\lfloor \frac{N}{J} \rfloor (j-1)+d,k} e^{j\phi_{\lfloor \frac{N}{J} \rfloor (j-1)+d,k}}, \end{aligned} \tag{2}$$

where $j \in \mathcal{J} \triangleq \{1, \ldots, J\}$ and $d \in \mathcal{D} \triangleq \{1, \ldots, \lfloor \frac{N}{J} \rfloor\}$ represent j-th reflection element part and d-th reflection element in j-th part, respectively. Meanwhile, k represents the transmit antenna combination selected from M_T. So the channel between the specified transmit antenna combination and j-th part of the RIS is given by:

$$\boldsymbol{h}_{kj} = \begin{bmatrix} h_{\lfloor \frac{N}{J} \rfloor (j-1)+1,k_{(1)}} + \cdots + h_{\lfloor \frac{N}{J} \rfloor (j-1)+1,k_{(J)}} \\ h_{\lfloor \frac{N}{J} \rfloor (j-1)+2,k_{(1)}} + \cdots + h_{\lfloor \frac{N}{J} \rfloor (j-1)+2,k_{(J)}} \\ \vdots \\ h_{\lfloor \frac{N}{J} \rfloor j,k_{(1)}} + \cdots + h_{\lfloor \frac{N}{J} \rfloor j,k_{(J)}} \end{bmatrix}. \tag{3}$$

The sub-channel $\mathbf{G}_j$ between j-th part of the RIS and the receiver is given in (4), as shown at the bottom of this page. Then, the j-th part reflection matrix designed for the specified transmit antennas and n_R-th selected receive antenna is expressed as:

$$\boldsymbol{\Theta}_{kj}^{n_R} = \operatorname{diag}\left[e^{j\theta^{n_R}_{k,\lfloor \frac{N}{J} \rfloor (j-1)+1}} \quad e^{j\theta^{n_R}_{k,\lfloor \frac{N}{J} \rfloor (j-1)+2}} \quad \ldots \quad e^{j\theta^{n_R}_{k,\lfloor \frac{N}{J} \rfloor j}} \right], \tag{5}$$

where $e^{j\theta^{n_R}_{k,\lfloor \frac{N}{J} \rfloor (j-1)+d}}$ represents the adjusted phase for the $\lfloor \frac{N}{J} \rfloor (j-1)+d$-th reflection element of the RIS. When N is large, and according to the Central limit Theorem (CLT), the received signal vector $\boldsymbol{y}$ can be expressed as:

$$\boldsymbol{y} = \frac{1}{\sqrt{N}} \sum_{j=1}^{J} \sqrt{\frac{E_s}{J}} \mathbf{G}_j \boldsymbol{\Theta}_{kj}^{n_R} \boldsymbol{h}_{kj} + \boldsymbol{n}, \tag{6}$$

where E_s is the transmitted signal energy and $\boldsymbol{n}$ is the Additive White Gaussian Noise (AWGN) term in which each entry has zero-mean and variance N_0. The expansion of the received signal vector $\boldsymbol{y}$ without AWGN term is given in (7), as shown at the top of next page. To maximize $\boldsymbol{y}$, the reflection coefficients need to satisfy

$$\theta^{n_R}_{k,\lfloor \frac{N}{J} \rfloor (j-1)+d} = -\phi_{\lfloor \frac{N}{J} \rfloor (j-1)+d,k} - \varphi_{n_R,\lfloor \frac{N}{J} \rfloor (j-1)+d} \tag{8}$$

determined by the specified transmit antennas and n_R-th receive antenna. After that, an optimal ML detector is considered for RIS-JTRSSK as follows:

$$[\hat{k}, \hat{z}] = \arg\min_{k,z} \{ |\boldsymbol{y} - \frac{1}{\sqrt{N}} \sum_{j=1}^{J} \sqrt{\frac{E_s}{J}} \mathbf{G}_j \boldsymbol{\Theta}_{\hat{k}j}^{n_R} \boldsymbol{h}_{\hat{k}j}| \}, \tag{9}$$

where z represents the receive antenna combination selected from M_R, denoted as $z = \{n_{R(1)}, ..., n_{R(j)}, ..., n_{R(J)}\}$, while $\hat{k}$ and $\hat{z}$ stand for the estimated transmit antenna combination and the estimated receive antenna combination, respectively.

B. Transmission Design with Imperfect CSI

Since the perfect CSI is usually difficult to obtain in practical, due to the complicated process of the channel estimation. We investigate the channel uncertainty scenarios under the bounded CSI error model for RIS-JTRSSK scheme. Specifically, we study the transmission design based on the IRRC and ICTRRC, respectively.

1) Scenario 1-IRRC: Considering the transmitter and the RIS are connected with each other through the RIS controller, we assume that the perfect CSI of the channel between the transmitter and the IRS is available. Based on this reasonable assumption and the framework of robust transmission design proposed in [34], the general imperfect CSI mode of the channel between the RIS and the receiver G_j can be expressed as:

$$G_j = \hat{G}_j + \Delta G_j, \forall j \in \mathcal{J}, \tag{10}$$

[3]In this paper, we aim to investigate the overall system performance of the proposed scheme to provide a technical foundation for its future extensions and applications. Therefore, we have adopted a general expression to calculate the SE of the system. Based on specific system requirements, the proposed scheme can be extended to a variable-rate system.

$$\mathbf{G}_j = \begin{bmatrix} \beta_{1,\lfloor \frac{N}{J} \rfloor (j-1)+1} e^{j\varphi_{1,\lfloor \frac{N}{J} \rfloor (j-1)+1}} & \beta_{1,\lfloor \frac{N}{J} \rfloor (j-1)+2} e^{j\varphi_{1,\lfloor \frac{N}{J} \rfloor (j-1)+2}} & \cdots & \beta_{1,\lfloor \frac{N}{J} \rfloor j} e^{j\varphi_{1,\lfloor \frac{N}{J} \rfloor j}} \\ \beta_{2,\lfloor \frac{N}{J} \rfloor (j-1)+1} e^{j\varphi_{2,\lfloor \frac{N}{J} \rfloor (j-1)+1}} & \beta_{2,\lfloor \frac{N}{J} \rfloor (j-1)+2} e^{j\varphi_{2,\lfloor \frac{N}{J} \rfloor (j-1)+2}} & \cdots & \beta_{2,\lfloor \frac{N}{J} \rfloor j} e^{j\varphi_{2,\lfloor \frac{N}{J} \rfloor j}} \\ \vdots & \vdots & \ddots & \vdots \\ \beta_{N_R,\lfloor \frac{N}{J} \rfloor (j-1)+1} e^{j\varphi_{N_R,\lfloor \frac{N}{J} \rfloor (j-1)+1}} & \beta_{N_R,\lfloor \frac{N}{J} \rfloor (j-1)+2} e^{j\varphi_{N_R,\lfloor \frac{N}{J} \rfloor (j-1)+2}} & \cdots & \beta_{N_R,\lfloor \frac{N}{J} \rfloor j} e^{j\varphi_{N_R,\lfloor \frac{N}{J} \rfloor j}} \end{bmatrix}. \tag{4}$$

Authorized licensed use limited to: University of Waterloo. Downloaded on March 25,2026 at 00:16:41 UTC from IEEE Xplore. Restrictions apply.
© 2026 IEEE. All rights reserved, including rights for text and data mining and training of artificial intelligence and similar technologies. Personal use is permitted, but republication/redistribution requires IEEE permission. See https://www.ieee.org/publications/rights/index.html for more information.

This article has been accepted for publication in IEEE Transactions on Vehicular Technology. This is the author's version which has not been fully edited and content may change prior to final publication. Citation information: DOI 10.1109/TVT.2026.3661626

$$\begin{aligned}\boldsymbol{y} &= \frac{1}{\sqrt{N}}\sum_{j=1}^{J}\sqrt{\frac{E_s}{J}}\mathbf{G}_j\boldsymbol{\Theta}_{kj}^{n_R}\boldsymbol{h}_{kj} \\ &= \frac{1}{\sqrt{N}}\sqrt{\frac{E_s}{J}}\sum_{j=1}^{J}\begin{bmatrix} \sum_{d=1}^{\lfloor \frac{N}{J}\rfloor}\beta_{1,\lfloor \frac{N}{J}\rfloor(j-1)+d}e^{j\varphi_{1,\lfloor \frac{N}{J}\rfloor(j-1)+d}}e^{j\theta_{k,\lfloor \frac{N}{J}\rfloor(j-1)+d}^{n_R}}(h_{\lfloor \frac{N}{J}\rfloor(j-1)+d,k_{(1)}}+\cdots+h_{\lfloor \frac{N}{J}\rfloor(j-1)+d,k_{(J)}}) \\ \sum_{d=1}^{\lfloor \frac{N}{J}\rfloor}\beta_{2,\lfloor \frac{N}{J}\rfloor(j-1)+d}e^{j\varphi_{2,\lfloor \frac{N}{J}\rfloor(j-1)+d}}e^{j\theta_{k,\lfloor \frac{N}{J}\rfloor(j-1)+d}^{n_R}}(h_{\lfloor \frac{N}{J}\rfloor(j-1)+d,k_{(1)}}+\cdots+h_{\lfloor \frac{N}{J}\rfloor(j-1)+d,k_{(J)}}) \\ \vdots \\ \sum_{d=1}^{\lfloor \frac{N}{J}\rfloor}\beta_{N_R,\lfloor \frac{N}{J}\rfloor(j-1)+d}e^{j\varphi_{N_R,\lfloor \frac{N}{J}\rfloor(j-1)+d}}e^{j\theta_{k,\lfloor \frac{N}{J}\rfloor(j-1)+d}^{n_R}}(h_{\lfloor \frac{N}{J}\rfloor(j-1)+d,k_{(1)}}+\cdots+h_{\lfloor \frac{N}{J}\rfloor(j-1)+d,k_{(J)}}) \end{bmatrix}. \end{aligned} \tag{7}$$

where $\hat{G}_j$ represents the correctly estimated channel, and $\Delta G_j \in \mathbb{C}^{N_r\times N}$ represents the corresponding CSI uncertainty error while it needs to satisfy the condition:

$$||\Delta G_j||_F \le \epsilon_j = \delta||\hat{G}_j||, \tag{11}$$

where ϵ_j is the bound of CSI uncertainty error and δ denotes the relative amount of CSI uncertainty. Therefore, by defining G_j with uncertainty error, the received signal vector $\mathbf{y}$ under imperfect CSI can be obtained from (6).

2) Scenario 2-ICTRRC: In complex electromagnetic environment, the accurate ICTRRC is also challenging to obtain. In this case, we assume that perfect CSI of the ICTRRC can not be obtained. Therefore, based on (6), the received signal vector $\boldsymbol{y}$ can be rewritten as:

$$\begin{aligned}\boldsymbol{y} &= \frac{1}{\sqrt{N}}\sum_{j=1}^{J}\sqrt{E_s}\mathbf{G}_j\boldsymbol{\Theta}_{kj}^{n_R}\boldsymbol{h}_{kj}+\boldsymbol{n}, \\ &= \frac{1}{\sqrt{N}}\sum_{j=1}^{J}\sqrt{E_s}\mathbf{T}_j\boldsymbol{\Phi}_{kj}^{n_R}+\boldsymbol{n}. \end{aligned} \tag{12}$$

where $\mathbf{T}_j$ is the cascaded channel from the transmitter to the receiver via the RIS, which can be expressed as $\mathbf{T}_j = \mathbf{G}_j\text{diag}(\boldsymbol{h}_{kj})$, and $\boldsymbol{\Phi}_{kj}^{n_R}$ is the vector containing diagonal elements of matrix $\boldsymbol{\Theta}_{kj}^{n_R}$, which can be represented as:

$$\boldsymbol{\Phi}_{kj}^{n_R} = [e^{j\theta_{k,\lfloor \frac{N}{J}\rfloor(j-1)+1}^{n_R}},\ldots,e^{j\theta_{k,\lfloor \frac{N}{J}\rfloor j}^{n_R}}]^T \in \mathbb{C}^{N\times 1}. \tag{13}$$

Moving a step further, considering the channel estimation error $||\Delta\mathbf{T}_j||_F \le \epsilon_j = \delta||\hat{\mathbf{T}}_j||$ with $\hat{\mathbf{T}}_j$ denoting the correctly estimated cascaded channel. Therefore, the actual channel is expressed as $\mathbf{T}_j = \hat{\mathbf{T}}_j + \Delta\mathbf{T}_j$.

Based on these two scenarios, the transmission design with imperfect CSI can also use ML detector to detect.[4]

III. Performance Analysis

In this section, the theoretical BER of the proposed RIS-JTRSSK scheme is investigated. We use optimal ML detector presented in the previous section to calculate the Pairwise Error Probability (PEP) for each combinations. Therefore, the PEP is shown as follows:

$$\begin{aligned} &P(k,z\to\hat{k},\hat{z}) \\ &=P\left(\left\|\boldsymbol{y}-\frac{\sum_{j=1}^{J}\sqrt{E_s}\mathbf{G}_j\boldsymbol{\Theta}_{kj}^{n_R}\boldsymbol{h}_{kj}}{\sqrt{N}}\right\|^2 > \left\|\boldsymbol{y}-\frac{\sum_{j=1}^{J}\sqrt{E_s}\mathbf{G}_j\boldsymbol{\Theta}_{\hat{k}j}^{\hat{n_R}}\boldsymbol{h}_{\hat{k}j}}{\sqrt{N}}\right\|^2\right) \\ &=P(V>0). \end{aligned} \tag{14}$$

Here, $V \sim \mathcal{N}(\mu_V,\sigma_V^2)$ with $\mu_V = -\Gamma$ and $\sigma_V^2 = 2N_0\Gamma$, where Γ is defined as:

$$\Gamma = \left\|\sum_{j=1}^{J}\mathbf{G}_j\boldsymbol{\Theta}_{kj}^{n_R}\boldsymbol{h}_{kj}-\sum_{j=1}^{J}\mathbf{G}_j\boldsymbol{\Theta}_{\hat{k}j}^{\hat{n_R}}\boldsymbol{h}_{\hat{k}j}\right\|^2. \tag{15}$$

Consequently, from $P(V>0) = Q(-\mu_V/\sigma_V)$, we have

$$P(k,z\to\hat{k},\hat{z}) = Q\left(\sqrt{\frac{\Gamma}{2N_0N}}\right). \tag{16}$$

Then, the average PEP (APEP) can be obtained by (16), yielding:

$$\bar{P}(k,z\to\hat{k},\hat{z}) = \int_0^\infty Q\left(\sqrt{\frac{\Gamma}{2N_0N}}\right)f_\Gamma(\Gamma)d\Gamma. \tag{17}$$

For simplicity, the APEP is computed using the Moment Generating Function (MGF) of Γ, which can be expressed as:

$$\begin{aligned}\bar{P}(k,z\to\hat{k},\hat{z}) &= \int_0^\infty Q\left(\sqrt{\frac{\Gamma}{2N_0N}}\right)f_\Gamma(\Gamma)d\Gamma. \\ &= \int_0^\infty\frac{1}{\pi}\int_0^{\pi/2}\exp\left(\frac{-\Gamma}{4\sin^2\eta N_0N}\right)f_\Gamma(\Gamma)d\eta d\Gamma. \\ &= \frac{1}{\pi}\int_0^{\pi/2}M_\Gamma\left(\frac{-E_s}{4N_0N\sin^2\eta}\right)d\eta. \end{aligned} \tag{18}$$

Moving a step further, we assume that the j-th part of the RIS specifies n_R-th antenna of the receiver. By adjusting the phase shifts of j-th part of the RIS, the phase of the correspondingly cascaded channel is tuned to be coherent. It is noteworthy that different antenna pairs selected at the

[4]In this paper, we aim to demonstrate the system performance of the proposed scheme under imperfect CSI conditions to investigate its practical applicability. The corresponding theoretical analysis for imperfect CSI scenarios can be built upon the frameworks established in [42] and [43].

Authorized licensed use limited to: University of Waterloo. Downloaded on March 25,2026 at 00:16:41 UTC from IEEE Xplore. Restrictions apply.
© 2026 IEEE. All rights reserved, including rights for text and data mining and training of artificial intelligence and similar technologies. Personal use is permitted, but republication/redistribution requires IEEE permission. See https://www.ieee.org/publications/rights/index.html for more information.

This article has been accepted for publication in IEEE Transactions on Vehicular Technology. This is the author's version which has not been fully edited and content may change prior to final publication. Citation information: DOI 10.1109/TVT.2026.3661626

$$\boldsymbol{t}_{kj}^{n_R} = \begin{bmatrix} \sum_{d=1}^{\lfloor \frac{N}{J} \rfloor} \beta_{1,\lfloor \frac{N}{J} \rfloor (j-1)+d} \alpha_{\lfloor \frac{N}{J} \rfloor (j-1)+d,k} e^{j(\theta^k_{1,\lfloor \frac{N}{J} \rfloor (j-1)+d} - \theta^k_{n_R,\lfloor \frac{N}{J} \rfloor (j-1)+d})} \\ \vdots \\ \sum_{d=1}^{\lfloor \frac{N}{J} \rfloor} \beta_{n_R,\lfloor \frac{N}{J} \rfloor (j-1)+d} \alpha_{\lfloor \frac{N}{J} \rfloor (j-1)+d,k} \\ \vdots \\ \sum_{d=1}^{\lfloor \frac{N}{J} \rfloor} \beta_{N_R,\lfloor \frac{N}{J} \rfloor (j-1)+d} \alpha_{\lfloor \frac{N}{J} \rfloor (j-1)+d,k} e^{j(\theta^k_{N_R,\lfloor \frac{N}{J} \rfloor (j-1)+d} - \theta^k_{n_R,\lfloor \frac{N}{J} \rfloor (j-1)+d})} \end{bmatrix}, \tag{19}$$

$$\boldsymbol{t}_{\hat{k}j}^{\hat{nR}} = \begin{bmatrix} \sum_{d=1}^{\lfloor \frac{N}{J} \rfloor} \beta_{1,\lfloor \frac{N}{J} \rfloor (j-1)+d} \alpha_{\lfloor \frac{N}{J} \rfloor (j-1)+d,\hat{k}} e^{j(\theta^{\hat{k}}_{1,\lfloor \frac{N}{J} \rfloor (j-1)+d} - \theta^{\hat{k}}_{\hat{nR},\lfloor \frac{N}{J} \rfloor (j-1)+d})} \\ \vdots \\ \sum_{d=1}^{\lfloor \frac{N}{J} \rfloor} \beta_{\hat{nR},\lfloor \frac{N}{J} \rfloor (j-1)+d} \alpha_{\lfloor \frac{N}{J} \rfloor (j-1)+d,\hat{k}} \\ \vdots \\ \sum_{d=1}^{\lfloor \frac{N}{J} \rfloor} \beta_{N_R,\lfloor \frac{N}{J} \rfloor (j-1)+d} \alpha_{\lfloor \frac{N}{J} \rfloor (j-1)+d,\hat{k}} e^{j(\theta^{\hat{k}}_{N_R,\lfloor \frac{N}{J} \rfloor (j-1)+d} - \theta^{\hat{k}}_{\hat{nR},\lfloor \frac{N}{J} \rfloor (j-1)+d})} \end{bmatrix}. \tag{20}$$

transmitter and the receiver correspond to distinct phase shifts in the respective channels. In other words, the chosen combination of transmit and receive antennas can be represented by the phase of the corresponding cascaded channel. Therefore, the cascaded channel between j-th part of the RIS and different transmit and receive antenna combining schemes, $\boldsymbol{t}_{kj}^{n_R}$ and $\boldsymbol{t}_{\hat{k}j}^{\hat{nR}}$, can be respectively expressed in (19) and (20) shown at the top of this page. For simplicity, we focus on handling the specified j-th part of the RIS and thus omitting $\lfloor \frac{N}{J} \rfloor (j-1)$ in the subscripts. Then, by defining $\bar{\boldsymbol{\Gamma}} = \sum_{j=1}^{J} \bar{\Gamma}_j \triangleq \sum_{j=1}^{J} \left(\boldsymbol{t}_{kj}^{n_R} - \boldsymbol{t}_{\hat{k}j}^{\hat{nR}} \right)$, $\bar{\Gamma}_j$ has the form of

$$\begin{bmatrix} \sum_n \beta_{1,n} \left(\alpha_{n,k} e^{j(\theta^k_{1,n} - \theta^k_{n_R,n})} - \alpha_{n,\hat{k}} e^{j(\theta^{\hat{k}}_{1,n} - \theta^{\hat{k}}_{\hat{nR},n})} \right) \\ \vdots \\ \sum_n \beta_{n_R,n} \left(\alpha_{n,k} - \alpha_{n,\hat{k}} e^{j(\theta^k_{n_R,n} - \theta^{\hat{k}}_{\hat{nR},n})} \right) \\ \vdots \\ \sum_n \beta_{\hat{nR},n} \left(\alpha_{n,k} e^{j(\theta^{\hat{k}}_{\hat{nR},n} - \theta^k_{n_R,n})} - \alpha_{n,\hat{k}} \right) \\ \vdots \\ \sum_n \beta_{N_R,n} \left(\alpha_{n,k} e^{j(\theta^k_{N_R,n} - \theta^k_{n_R,n})} - \alpha_{n,\hat{k}} e^{j(\theta^{\hat{k}}_{N_R,n} - \theta^{\hat{k}}_{\hat{nR},n})} \right) \end{bmatrix}. \tag{21}$$

It is obvious that only n_R-th row and $\hat{nR}$-th row are not independent. After tedious mathematical calculations, the distributions of $\bar{\Gamma}_{jR}$ and $\bar{\Gamma}_{jR}$ except for the n_R-th row and $\hat{nR}$-th row follow $\mathcal{N}(0, N_g)$, where $N_g = \lfloor \frac{N}{J} \rfloor$.[5] To step further, we treat the terms in n_R-th row and $\hat{nR}$-th row, $\bar{\Gamma}_{j(n_R,n)}$ and $\bar{\Gamma}_{j(\hat{nR},n)}$, as the combination of real part and imaginary part, respectively, i.e., $\bar{\Gamma}_{j(n_R,n)} = \bar{\Gamma}_{j(n_R,n)R} + j\bar{\Gamma}_{j(n_R,n)I}$ and $\bar{\Gamma}_{j(\hat{nR},n)} = \bar{\Gamma}_{j(\hat{nR},n)R} + j\bar{\Gamma}_{j(\hat{nR},n)I}$. By defining $\mathbb{U} \triangleq \{1, 2, ..., N_R\}$ and $\mathbb{U}_{\mathbb{R}} \triangleq \{n_R, \hat{nR}\}$, it can be easily seen that $\bar{\Gamma}_{j(u,n)}, \forall u \in \mathbb{U}_{\mathbb{R}}{}^c \triangleq \{u \in \mathbb{U} : u \notin \mathbb{U}_{\mathbb{R}}\}, \forall n \in \mathcal{N} \triangleq \{1, \ldots, N\}$ are independent. According to the CLT, the real and imaginary parts of $\sum_{j=1}^{J} \bar{\Gamma}_{j(u)} = \sum_{j=1}^{J} \sum_{n=1}^{N} \bar{\Gamma}_{j(u,n)}$ follow the Gaussian distribution. Considering the $\mathbb{U}_{\mathbb{R}} = \{n_R, \hat{nR}\}$ case, $\bar{\Gamma}_{j(n_R,n)}$ and $\bar{\Gamma}_{j(\hat{nR},n)}$ are not independent of each other. To this end, we first calculate the mean $\boldsymbol{m}$ and covariance $\mathbf{C}$ of $\boldsymbol{x} = [\sum_{j=1}^{J} \bar{\Gamma}_{j(n_R)R}, \sum_{j=1}^{J} \bar{\Gamma}_{j(n_R)I}, \sum_{j=1}^{J} \bar{\Gamma}_{j(\hat{nR})R}, \sum_{j=1}^{J} \bar{\Gamma}_{j(\hat{nR})I}]^T$, as follows:

$$\boldsymbol{m} = N_g [\frac{\pi}{4}, 0, -\frac{\pi}{4}, 0]^T, \tag{22}$$

$$\mathbf{C} = N_g \begin{bmatrix} \frac{24-\pi^2}{16} & 0 & -\frac{\pi^2}{32} & 0 \\ 0 & \frac{1}{2} & 0 & \frac{\pi^2}{32} \\ -\frac{\pi^2}{32} & 0 & \frac{24-\pi^2}{16} & 0 \\ 0 & \frac{\pi^2}{32} & 0 & \frac{1}{2} \end{bmatrix}. \tag{23}$$

From [10, eq. 31], the MGF of $\bar{\Gamma}$ can be expressed as

$$M_{\bar{\Gamma}}(s) = (\det(\mathbf{I} - 2s\mathbf{A}\mathbf{C}_{\bar{\Gamma}}))^{(-1/2)} \times \exp\left(-\frac{1}{2} \boldsymbol{m}_{\bar{\Gamma}}^T \left[\mathbf{I} - (\mathbf{I} - 2s\mathbf{A}\mathbf{C}_{\bar{\Gamma}})^{-1} \right] \mathbf{C}_{\bar{\Gamma}}^{-1} \boldsymbol{m}_{\bar{\Gamma}} \right), \tag{24}$$

where

$$\boldsymbol{m}_{\bar{\Gamma}} = \begin{bmatrix} \sum_{j=1}^{J} m(\bar{\Gamma}_{j(1)R}) \\ \sum_{j=1}^{J} m(\bar{\Gamma}_{j(1)I}) \\ \vdots \\ \sum_{j=1}^{J} m(\bar{\Gamma}_{j(N_R)R}) \\ \sum_{j=1}^{J} m(\bar{\Gamma}_{j(N_R)I}) \end{bmatrix}, \tag{25}$$

[5]The channel coefficients α and β are independent Random Variables (RVs) that follow a Rayleigh distribution, with the corresponding normal distribution parameters of $\mathcal{N}\left(\frac{\sqrt{\pi}}{2}, \frac{4-\pi}{4}\right)$. Meanwhile, both the real and imaginary components of the uniformly distributed phase θ conform to the normal distribution $\mathcal{N}\left(0, \frac{1}{2}\right)$. By applying the calculation rules for the mean and variance of RVs, the probability distribution of $\bar{\Gamma}_j$ can be derived accordingly.

Authorized licensed use limited to: University of Waterloo. Downloaded on March 25,2026 at 00:16:41 UTC from IEEE Xplore. Restrictions apply.
© 2026 IEEE. All rights reserved, including rights for text and data mining and training of artificial intelligence and similar technologies. Personal use is permitted, but republication/redistribution requires IEEE permission. See https://www.ieee.org/publications/rights/index.html for more information.

This article has been accepted for publication in IEEE Transactions on Vehicular Technology. This is the author's version which has not been fully edited and content may change prior to final publication. Citation information: DOI 10.1109/TVT.2026.3661626

$$\mathbf{C}_{\bar{\Gamma}} = \begin{bmatrix} \sum_{j=1}^{J} c(\bar{\Gamma}_{j(1)R}, \bar{\Gamma}_{j(1)R}) & \cdots & \sum_{j=1}^{J} c(\bar{\Gamma}_{j(1)R}, \bar{\Gamma}_{j(N_R)I}) \\ \vdots & \ddots & \vdots \\ \sum_{j=1}^{J} c(\bar{\Gamma}_{j(N_R)R}, \bar{\Gamma}_{j(1)R}) & \cdots & \sum_{j=1}^{J} c(\bar{\Gamma}_{j(N_R)R}, \bar{\Gamma}_{j(N_R)I}) \end{bmatrix} \tag{26}$$

where each entry of (25) and (26) can be obtained, according to (22) and (23). Combining (18) and (22)-(26), the following union bound on ABER can be written as:

$$P \leq \sum_{k} \sum_{n_R} \sum_{\hat{k}} \sum_{\hat{n_R}} \bar{P}(k, z \to \hat{k}, \hat{z}) \times \frac{d(k, z \to \hat{k}, \hat{z})}{S_T S_R \frac{N_L}{2} (\log_2 S_T + \log_2 S_R + \log_2 \frac{N_L}{2})}, \tag{27}$$

where $d(k, z \to \hat{k}, \hat{z})$ denotes the number of bits in error for the corresponding pairwise error event.

IV. Different Bit Matching Mechanism for RIS-JTRSSK

In the RIS-JTRSSK scheme, the first b_1 bit part determines the number of activated antennas at the transmitter and receiver. Therefore, the same number of antennas are activated at transmitter and receiver in each time slot. To further improve the SE of the system, we change the bit matching mechanism of RIS-JTRSSK scheme so that the number of activated antennas at the transmitter and the receiver are determined by different bit parts, which is named RIS-FTRSSK scheme and the system model is presented in Fig. 2. Specifically, the incoming bits are divided into four parts, i.e., l_1, l_2, l_3, and l_4. The first l_1 bit group determines the number of antennas activated by the transmitter, which is denoted as A_T and it ranges from 1 to N_T/2. The third l_3 bit group determines the number of antennas activated by the receiver, which is denoted as A_R and it ranges from 1 to N_R/2. The matching principle of the remaining two bit groups l_2 and l_4 is consistent with the matching principle of b_2 and b_3 mentioned in the Section II. Therefore, the SE of RIS-FTRSSK scheme can be calculated by:

$$r_f = \log_2(\frac{N_T}{2}) + \log_2(S_T) + \log_2(\frac{N_R}{2}) + \log_2(S_R). \tag{28}$$

The number of transmit antenna combinations and receive antenna combinations can be calculated as $F_T = \binom{N_T}{A_T}$ and $F_R = \binom{N_R}{A_R}$, respectively. So the channel between the specified g transmit antennas and specified A_r-th part of the RIS can be rewritten as:

$$\boldsymbol{h}_{gA_r} = \begin{bmatrix} h_{\lfloor \frac{N}{A_R} \rfloor (A_r-1)+1, g_{(1)}} + \cdots + h_{\lfloor \frac{N}{A_R} \rfloor (A_r-1)+1, g_{(A_T)}} \\ h_{\lfloor \frac{N}{A_R} \rfloor (A_r-1)+2, g_{(1)}} + \cdots + h_{\lfloor \frac{N}{A_R} \rfloor (A_r-1)+2, g_{(A_T)}} \\ \vdots \\ h_{\lfloor \frac{N}{A_R} \rfloor A_r, g_{(1)}} + \cdots + h_{\lfloor \frac{N}{A_R} \rfloor A_r, g_{(A_T)}} \end{bmatrix}, \tag{29}$$

where $A_r \in \{1, 2, \ldots, A_R\}$. Based on the equation expression given in (4) and (5), we can obtain the Rayleigh sub-channel $\mathbf{G}_{A_r}$ between the A_r-th part of the RIS and the receiver as well as the A_r-th part reflection matrix $\boldsymbol{\Theta}_{gA_r}^{n_R}$. Therefore, the received signal vector $\boldsymbol{y}$ can be expressed as:

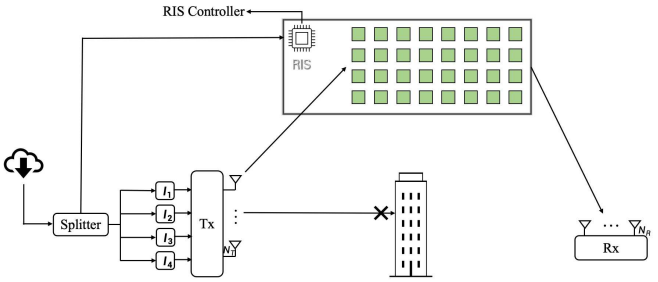

Fig. 2. System model for the proposed RIS-FTRSSK scheme.

$$\boldsymbol{y} = \frac{1}{\sqrt{N}} \sum_{A_r=1}^{A_R} \sqrt{E_s} \mathbf{G}_{A_r} \boldsymbol{\Theta}_{gA_r}^{n_R} \boldsymbol{h}_{gA_r} + \boldsymbol{n}. \tag{30}$$

Then, an optimal ML detector can be designed by utilizing (9) as follows:

$$[\hat{g}, \hat{z}] = \arg \min_{g,z} \{ |\boldsymbol{y} - \frac{1}{\sqrt{N}} \sum_{A_r=1}^{A_R} \sqrt{E_s} \mathbf{G}_{A_r} \boldsymbol{\Theta}_{\hat{g}A_r}^{\hat{n}_R} \boldsymbol{h}_{\hat{g}A_r} | \}. \tag{31}$$

Compared with RIS-JTRSSK scheme, RIS-FTRSSK scheme can transmit more bits under the same antenna setting, which can be regarded as a transmission scheme for achieving a higher SE. These two schemes can be consider as a generalized scheme of RIS-assisted SSK modulation. In order to understand the process of matching mechanism more clearly, an example is illustrated for RIS-FTRSSK scheme with N_T = 4 and N_R = 4.

Example: In this case, A_T and A_R have values ranging from 1 to 2 with N_T = 4 and N_R = 4, therefore, l_1 and l_3 can be calculated as one bit, respectively. When A_T = A_R = 1, the transmit antenna combination F_T and receive antenna combination F_R are four. When A_T = A_R = 2, the F_T and F_R are six. Because the number of selected antenna combinations must be power of two, therefore, we randomly select four antenna combinations out of F_T and F_R, respectively. Then, the SE of RIS-FTRSSK scheme r_f is 6 bits/s/Hz and the mapping table is shown in Table II. Assume that the incoming bits are 010110, which are separated into four subgroups as l_1 = 0, l_2 = 10, l_3 = 1, and l_4 = 10. According to Table II, the transmitter activates one antenna and the receiver activates two antennas when l_1 = 0 and l_3 = 1. When l_2 = 10 and l_4 = 10, the third transmit antenna is selected by the transmitter and the third receive antenna combination is selected by the receiver. In this way, the information bits 010110 are conveyed by RIS-FTRSSK scheme.

V. Antenna Selection Aided RIS-JTRSSK

In this section, we extend our design to the RIS-JTRSSK with Antenna Selection (RIS-AS-JTRSSK) scheme in order to achieve further diversity gain. In addition, an FEA is also proposed to implement lower selection complexity.

Authorized licensed use limited to: University of Waterloo. Downloaded on March 25,2026 at 00:16:41 UTC from IEEE Xplore. Restrictions apply.
© 2026 IEEE. All rights reserved, including rights for text and data mining and training of artificial intelligence and similar technologies. Personal use is permitted, but republication/redistribution requires IEEE permission. See https://www.ieee.org/publications/rights/index.html for more information.

This article has been accepted for publication in IEEE Transactions on Vehicular Technology. This is the author's version which has not been fully edited and content may change prior to final publication. Citation information: DOI 10.1109/TVT.2026.3661626

TABLE II
MAPPING FOR RIS-FTRSSK SCHEME WITH N_T = 4 and N_R = 4

l_1	Tx active antenna	l_2	Tx antenna combination
0	1	00	1-th
		01	2-th
		10	3-th
		11	4-th
1	2	00	(1,2)
		01	(2,4)
		10	(1,4)
		11	(3,4)
l_3	Rx active antenna	l_4	Rx antenna combination
0	1	00	1-th
		01	2-th
		10	3-th
		11	4-th
1	2	00	(1,3)
		01	(2,3)
		10	(2,4)
		11	(1,4)

A. RIS-AS-JTRSSK

Assume that the controller uses the CSI to select a subset $p = (k, z)$ to transmit information. Specifically, k represents transmit antenna index selected from M_T transmit antenna combinations, while z is the receive antenna index selected from M_R receive antenna combinations. Therefore, the received signal vector of the p-th antenna subset can be expressed as:

$$\begin{aligned}\boldsymbol{y}^p &= \frac{1}{\sqrt{N}}\sum_{j=1}^{J}\sqrt{E_s}\mathbf{G}_j^p\boldsymbol{\Theta}_{kj}^{n_R}\boldsymbol{h}_{kj}^p + \boldsymbol{n}^p \\ &\overset{\text{def}}{=} \frac{1}{\sqrt{N}}\mathbf{d}_{kz}^p + \boldsymbol{n}^p. \end{aligned} \tag{32}$$

where $\mathbf{d}_{kz}^p$ represents the instantaneous energy of p subset from the RIS.

As can be seen from (14), the instantaneous performance of a certain subset depends on the quality of the antenna pair. Therefore, we can use the principle of Maximizing Minimum Euclidean Distance (MMED) to select the antenna subset with the larger Euclidean distance, then we have the following function:

$$\begin{aligned} q(p) &= \min_{k,z,\hat{k},\hat{z}} \left\| \mathbf{d}_{kz}^p - \mathbf{d}_{\hat{k}\hat{z}}^{\hat{p}} \right\|^2, \\ \text{s.t.} &\begin{cases} k,\hat{k} & \in & 1,2,...,M_T \\ z,\hat{z} & \in & 1,2,...,M_R \end{cases}, \end{aligned} \tag{33}$$

where the constraint is $(k, z) \neq (\hat{k}, \hat{z})$. Let $\mathcal{P}$ represents the set of all possible subset and consider all possibilities, then the optimal subset $\hat{p}$ is obtained by:

$$\hat{p} = \arg\max_{p\in\mathcal{P}} q(p). \tag{34}$$

Following this, the subset $\hat{p}$ is removed from $\mathcal{P}$ and stored in the new set $\mathcal{V}$, while transmit antenna combination $\hat{k}$ and receive antenna combination $\hat{z}$ are removed from M_T and M_R, respectively. Then, repeating (33) and (34) for S - 1 times until generating other S - 1 subsets, where S is the number of selected subset.

Algorithm 1 Fast elimination algorithm

Input: $\mathbf{h}$, $\mathbf{G}$, N, N_T, N_R, M_T, M_R, N_0
Output: M_T, M_R

```
Define the number of active antennas J.
The corresponding transmit antenna combinations M_T and receive antenna combinations M_R are generated by J, respectively.
k = {1, 2, ..., M_T}
z = {1, 2, ..., M_R}
p = (k, z)
Define the number of n_t elements required in M_T.
Define the number of n_r elements required in M_R.
repeat
    Calculate q(p) = min || d_{kz}^p − d_{k̂ẑ}^{p̂} ||^2.
    Find (k_1, z_1 → k_2, z_2) according to q(p).
    Calculate Z_i(k_1, z_1) and Z_i(k_2, z_2) based on (35).
    (k̃, z̃) = arg min {Z_i(k_1, z_1), Z_i(k_2, z_2)}.
    M_T = M_T - {k̃}.
    M_R = M_R - {z̃}.
until M_T == n_t, M_R == n_r.
```

B. Fast elimination algorithm

Considering that when the number of subsets is large, the complexity of antenna selection is high. To reduce the complexity, we design an antenna selection based greedy elimination algorithm, which is named FEA. Specifically, we exploit the working principle of Signal-to-Leakage-and-Noise Ratio (SLNR) to determine the worst antenna combination pair, which can be written as:

$$Z_i(k,z) = \frac{|(\boldsymbol{w}_i)^T\mathbf{d}_{kz,j}|^2}{\sum\limits_{e,e\neq i}|(\boldsymbol{w}_i)^T\mathbf{d}_{kz,j}|^2 + NN_0}, \tag{35}$$

where $\boldsymbol{w}_i$ represents the i-th column of $\mathbf{E}_{M_R}$ and $i \in \{1, 2, ..., M_R\}$. Based on this, the worst antenna combination pair can be calculated as:

$$(\tilde{k},\tilde{z}) = \arg\min\{Z_i(k_1,z_1), Z_i(k_2,z_2)\}. \tag{36}$$

Then, we remove $\tilde{k}$-th transmit antenna combination from M_T and $\tilde{z}$-th receive antenna combination from M_R, respectively. Repeating the above steps until the number of elements in M_T and M_R is equal to n_t and n_r, respectively, where n_t and n_r indicate the required number of antenna combinations. The details of FEA is summarized in Algorithm 1.

VI. LOW-COMPLEXITY DETECTOR AND DETECTION COMPLEXITY ANALYSIS

Since the ML detector seeks all antenna combinations on the received signal vector $\boldsymbol{y}$, its complexity is undoubtedly high. Therefore, an LC detector combined with greedy algorithm is proposed, which can reduce the detection complexity of ML detector. In addition, the detection complexity of ML detector and LC detector are investigated.

Authorized licensed use limited to: University of Waterloo. Downloaded on March 25,2026 at 00:16:41 UTC from IEEE Xplore. Restrictions apply.
© 2026 IEEE. All rights reserved, including rights for text and data mining and training of artificial intelligence and similar technologies. Personal use is permitted, but republication/redistribution requires IEEE permission. See https://www.ieee.org/publications/rights/index.html for more information.

This article has been accepted for publication in IEEE Transactions on Vehicular Technology. This is the author's version which has not been fully edited and content may change prior to final publication. Citation information: DOI 10.1109/TVT.2026.3661626

TABLE III
DETECTION COMPLEXITY ANALYSIS SUMMARY

Scheme	Complexity
RIS-JTRSSK	$((\frac{9}{4}N_R+\frac{7}{4})N+N_R)2^r$
RIS-SM	$((2N_R+2)N+3N_R)N_TN_RM$
RIS-TRSSK	$((2N_R+2)N+N_R)N_TN_R$
RIS-TRGSSK	$((\frac{5}{2}N_R+2)N+N_R)2^m$

A. Low-complexity detector

First, we calculate the instantaneous energy of all receive antennas based on greedy algorithm when the K-th antenna combination is selected, where K-th antenna combination represents the subset of antenna combinations selected from M_T and M_R, respectively. Therefore, it can be calculated as:

$$\hat{\boldsymbol{a}}_K = \underset{m\in\{1,\dots,N_R\}}{\arg\,\text{sorted}}\ (|\boldsymbol{y}_{K,m}|^2), \tag{37}$$

where $\hat{\boldsymbol{a}}_K$ is a vector of sorted instantaneous energy $\boldsymbol{y}_{K,m}$ of all receive antennas in a descending order, while m and $\boldsymbol{y}_{K,m}$ represent m-th receive antenna and the received signal at the m-th antenna, respectively. Then, we select N_e receive antennas with maximum instantaneous energy from $\hat{a}_K$ and obtain a new vector $\boldsymbol{\kappa}$, where $N_e = (N_R + \frac{N_R}{2})/2$ and $\boldsymbol{\kappa} \in \mathbb{N}^{N_e\times 1}$.[6] When the N_e is determined, the new antenna combinations set corresponding to the remaining antennas in vector $\boldsymbol{\kappa}$ is denoted as v. From this, we use ML detector to detect selected antenna combination from set v, which can be expressed as follows:

$$\hat{\boldsymbol{v}} = \arg\min_{v} |\boldsymbol{y} - \hat{\boldsymbol{y}}_{\hat{v}}|^2, \tag{38}$$

where $\hat{\boldsymbol{y}}_{\hat{v}}$ represents the received signal of each corresponding antenna combinations from set v and $\hat{v}$ is the estimated antenna combination to convey information.

In this way, compared with the ML detector, the proposed detector has lower detection complexity, and the detection complexities of these two detectors are discussed in next subsection.

B. Detection complexity analysis

In this subsection, we present the computational complexity of the proposed scheme, which is calculated by the number of Complex Multiplications (CMs) and Complex Additions (CAs) required for ML detector in (9). Therefore, the complexity of RIS-JTRSSK scheme is give by:

$$C_{\text{ML,RIS-JTRSSK}} = ((\frac{\frac{N_R}{2}+1}{2}+1)N + (2N+1)N_R)2^r, \tag{39}$$

where $\frac{\frac{N_R}{2}+1}{2}$ is the expected value of J. Then, the complexity of the LC detector is also calculated by the number of CMs and CAs required in (38), which can be expressed as:

$$C_{\text{LCD}} = ((\frac{\frac{N_R}{2}+1}{2}+1)N + (2N+2)N_R)2^{\tilde{r}}, \tag{40}$$

[6]The number of N_e receive antennas is discussed in Section VI, and according to the simulation result, the proposed scheme with LC detector has the optimal system performance when $N_e = (N_R + \frac{N_R}{2})/2$.

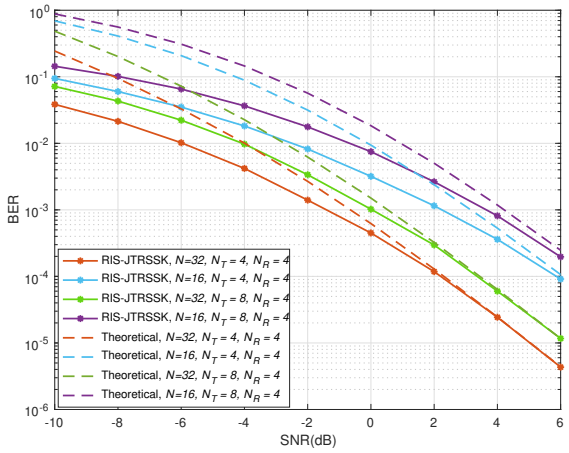

Fig. 3. The BER performance of RIS-JTRSSK scheme under different settings with increasing N.

where

$$\tilde{r} = \log(\frac{N_R}{2}) + \log(S_T) + \log(S_{Re}), \tag{41}$$

with S_{Re} being the number of antenna combinations selected from $M_{Re} = \binom{N_e}{J}$.

As can be seen from (39) and (40), the conventional ML detector and the LC detector require almost the same number of CMs and CAs for detecting an antenna combination, but the LC detector requires less number of receive antenna combinations based on greedy algorithm. Therefore, the proposed detector has lower computational complexity. To further demonstrate the performance of the LC detector, the BER performance and time complexities of these two detectors are investigated in Section VII.

Furthermore, the results of the complexity analysis based on ML detector are summarized in Table III, which also includes RIS-SM, RIS-TRSSK, and RIS-TRGSSK schemes. It is clear that RIS-SM scheme has the highest complexity, while RIS-JTRSSK, RIS-TRSSK, and RIS-TRGSSK schemes have almost the same lower complexity. But compared with our proposed RIS-JTRSSK scheme, the other two schemes require more number of antennas to achieve the same SE. Therefore, RIS-JTRSSK scheme not only has the lower detection complexity but also has the highest SE under the condition of the same antennas.

VII. SIMULATION RESULTS

In this section, we compare the BER performance and complexity of the proposed RIS-JTRSSK scheme using Monte Carlo simulation with RIS-SM, RIS-TRSSK and RIS-TRGSSK schemes. To ensure the accuracy of the experimental results, the SNR value is defined as E_s/N_0 and the total simulation bits are set as 2×10^5 for each SNR value. Our proposed optimization methods, i.e., antenna selection algorithm, FEA and LC algorithm, are also verified by the simulation results. In addition, in order to achieve the best performance of the proposed scheme, we set both S_T and S_R to the maximum values, i.e. N_T and N_R, respectively.

Authorized licensed use limited to: University of Waterloo. Downloaded on March 25,2026 at 00:16:41 UTC from IEEE Xplore. Restrictions apply.
© 2026 IEEE. All rights reserved, including rights for text and data mining and training of artificial intelligence and similar technologies. Personal use is permitted, but republication/redistribution requires IEEE permission. See https://www.ieee.org/publications/rights/index.html for more information.

This article has been accepted for publication in IEEE Transactions on Vehicular Technology. This is the author's version which has not been fully edited and content may change prior to final publication. Citation information: DOI 10.1109/TVT.2026.3661626

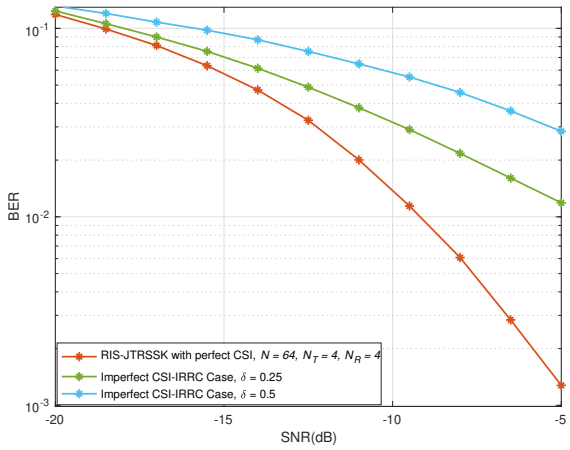

Fig. 4. The BER performance of RIS-JTRSSK scheme under IRRC case with $\delta = \{0.25, 0.5\}$.

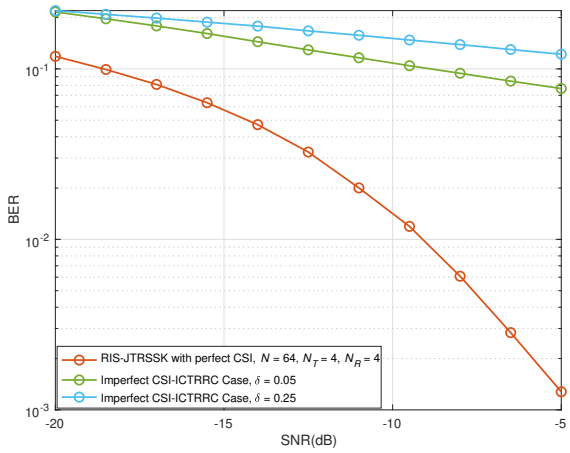

Fig. 5. The BER performance of RIS-JTRSSK scheme under ICTRRC case with increasing $\delta = \{0.05, 0.25\}$.

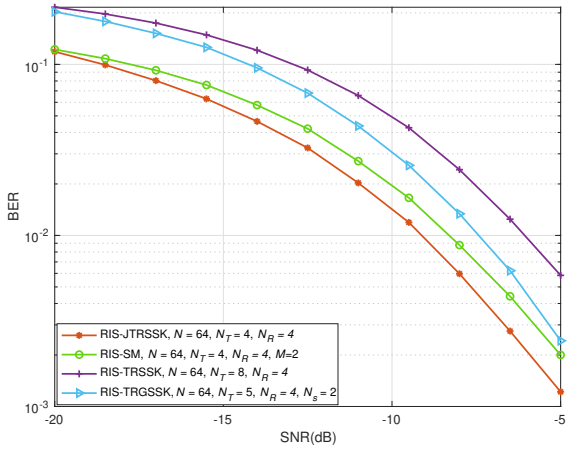

Fig. 6. Comparisons of BER performance in RIS-JTRSSK with RIS-SM, RIS-TRSSK and RIS-TRGSSK for 5 bits/s/Hz with N = 64.

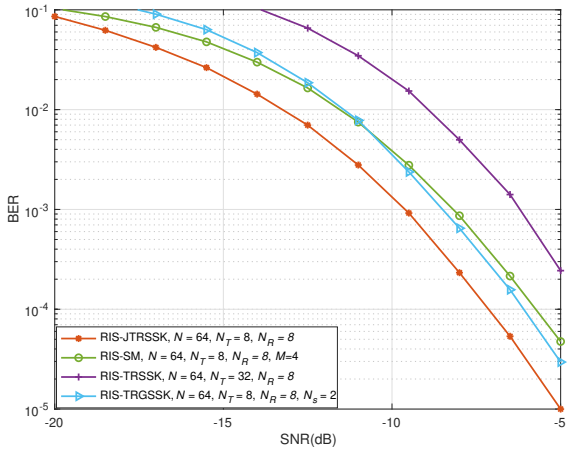

Fig. 7. Comparisons of BER performance in RIS-JTRSSK with RIS-SM, RIS-TRSSK and RIS-TRGSSK for 8 bits/s/Hz with N = 64.

Firstly, the BER performance of the proposed RIS-JTRSSK scheme is verified by the analytical derivations presented in Section III, which is shown in Fig. 3. According to this figure, in the same setting, the theoretical results extremely approach to the simulation results in higher SNR situation, especially when the number of reflection elements is larger. In addition, doubling the number of reflection elements N can bring 1.5 dB gains to achieve the same BER performance.

As shown in Fig. 4 and Fig. 5, we illustrate the BER performance of the proposed RIS-JTRSSK scheme under two types of imperfect channel cases, IRRC and ICTRRC, respectively. In the IRRC case, the channel uncertainty levels are chosen as $\delta = \{0.25, 0.5\}$. Compared with RIS-JTRSSK with perfect CSI case, it can lead to a performance decrease of approximate 4 dB and 7 dB under the equivalent BER performance. For the ICTRRC case, the channel uncertainty levels are chosen as $\delta = \{0.05, 0.25\}$. Compared with the IRRC case, the ICTRRC case has a more pronounced impact on the BER performance of the RIS-JTRSSK scheme, resulting in a performance degradation of approximate 12 dB at δ = 0.05. Therefore, the BER performance degrades as the channel uncertainty level increases, particularly in the high SNR region. The reason is that higher channel uncertainty level is related to a higher error in the channel estimation, which makes the ML detection more difficult.

Fig. 6 illustrates the comparison between the proposed scheme and other index modulation based schemes, where RIS-SM scheme was proposed in [32], and RIS-TRSSK and RIS-TRGSSK schemes are the benchmark schemes. Here, the benchmark schemes RIS-TRSSK and RIS-TRGSSK can be obtained by extending the system models in [16] and [19], respectively. In order to ensure the comparison as fair as possible, the number of receive antennas is set to be same for all schemes, and other parameters are changed according to the SE. It can be seen from the figure that RIS-JTRSSK scheme has the best BER performance, which can bring 1 dB, 2 dB and 4 dB gains compared with RIS-SM, RIS-TRGSSK and RIS-TRSSK under the same BER performance, respectively. Mean-

Authorized licensed use limited to: University of Waterloo. Downloaded on March 25,2026 at 00:16:41 UTC from IEEE Xplore. Restrictions apply.
© 2026 IEEE. All rights reserved, including rights for text and data mining and training of artificial intelligence and similar technologies. Personal use is permitted, but republication/redistribution requires IEEE permission. See https://www.ieee.org/publications/rights/index.html for more information.

This article has been accepted for publication in IEEE Transactions on Vehicular Technology. This is the author's version which has not been fully edited and content may change prior to final publication. Citation information: DOI 10.1109/TVT.2026.3661626

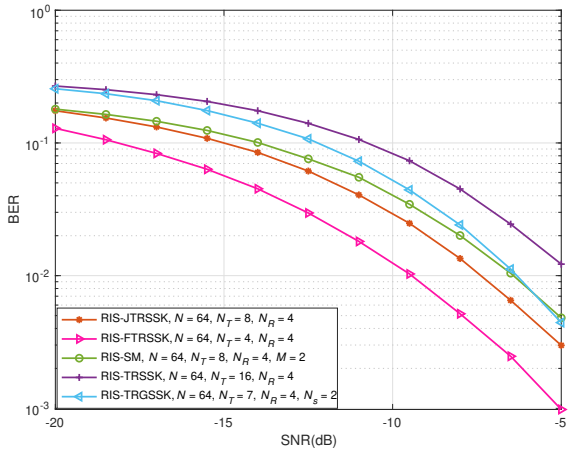

Fig. 8. Comparison of BER performance among RIS-FTRSSK, RIS-JTRSSK, RIS-SM, RIS-TRSSK and RIS-TRGSSK for 6 bits/s/Hz with N = 64.

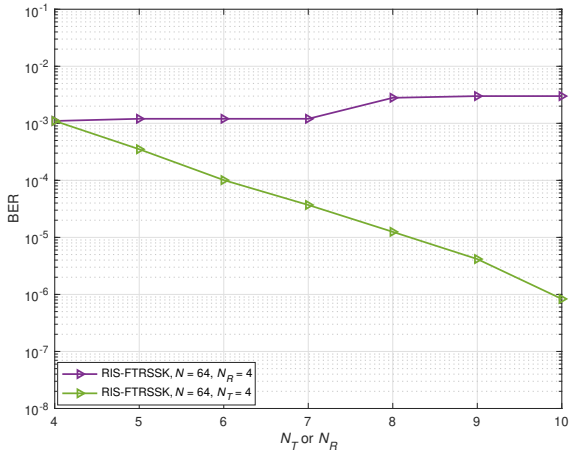

Fig. 9. The trend of BER performance when increasing transmit antennas or receive antennas under N = 64.

TABLE IV
THE COMPUTATIONAL COMPLEXITY OF RIS-AS-JTRSSK AND RIS-AS-JTRSSK WITH FEA

(N_T, N_R)	(n_t, n_r)	RIS-AS-JTRSSK	RIS-AS-JTRSSK with FEA
(8, 8)	(16, 16)	1330261	82688
(9, 9)	(24, 24)	3849984	217856

while, all competing schemes necessitate more parameters than the proposed scheme to achieve the identical SE. Then, we extend our analysis to SE = 8 bits/s/Hz, which is shown in Fig. 7. On the one hand, compared to RIS-JTRSSK, RIS-SM and RIS-TRSSK require additional antennas or higher symbol modulation orders to attain the same SE, thereby increasing the system complexity. On the other hand, for all SNR values, the results of RIS-JTRSSK performe better than the other three schemes, in terms of BER. Therefore, compared with all benchmark schemes, the proposed scheme achieves superior SE without requiring additional system configuration, further demonstrating its system flexibility.

Next, the BER performance of the RIS-FTRSSK, RIS-JTRSSK and other three reference schemes is compared under SE = 6 bits/s/Hz, as displayed in Fig. 8. With respect to the number of antennas, compared with other schemes, RIS-FTRSSK uses the least number of antennas to achieve the same SE. Moreover, RIS-FTRSSK exhibits the most favorable BER performance, yielding a 2 dB advantage over RIS-JTRSSK. Despite the exceptional performance exhibited by RIS-FTRSSK, its system model is relatively more complicated than those of the other schemes. If we only focus on the number of antennas and BER performance, RIS-FTRSSK can be considered as a good candidate scheme.

To illustrate the influence of increasing transmit antennas or receive antennas to the BER performance of RIS-JTRSSK, we provide the comparison of increasing antennas in Fig. 9 under N = 64, where the SNR value is fixed at -5 dB. First, it can be seen from the figure that when the receive antennas are fixed at 4 and the transmit antennas are increased from 4 to 10, the BER performance of RIS-JTRSSK presents a flat trend.

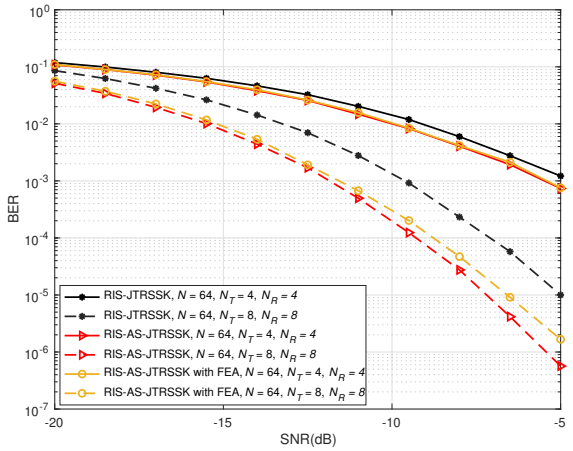

Fig. 10. Performance comparison of the RIS-JTRSSK, RIS-AS-JTRSSK and RIS-AS-JTRSSK with FEA for different values of N_T and N_R.

Therefore, in the comparison of previous simulation results, we set the number of receive antennas to be consistent and only change other variables to ensure fairness. Furthermore, the figure shows the inflection point at N_T = 8, and the reason is that the SE at the b_2 bit part becomes 3 bits based on $\log_2(N_T)$. Then, we fix the transmit antennas at 4 and the receive antennas are increased from 4 to 10. It is worth noting that when the number of receiver antennas is more than that of transmitter antennas, the matching mechanism of b_1 bits part will switch from $\frac{N_R}{2}$ to $\frac{N_T}{2}$. Following this, under the same SE, not only the dimension of the received signal vector y increases, but also the number of receive antenna combinations increases. According to the working principle of MMED and ML detector, the performance of BER is determined by the Euclidean distance between each antenna. Therefore, the BER performance of RIS-JTRSSK improves with the increase of receive antennas.

Fig. 10 shows the BER performance of RIS-AS-JTRSSK scheme and RIS-AS-JTRSSK with FEA in the two cases (N_T = 4, N_R = 4 and N_T = 8, N_R = 8). In the first case, the RIS-

Authorized licensed use limited to: University of Waterloo. Downloaded on March 25,2026 at 00:16:41 UTC from IEEE Xplore. Restrictions apply.
© 2026 IEEE. All rights reserved, including rights for text and data mining and training of artificial intelligence and similar technologies. Personal use is permitted, but republication/redistribution requires IEEE permission. See https://www.ieee.org/publications/rights/index.html for more information.

This article has been accepted for publication in IEEE Transactions on Vehicular Technology. This is the author's version which has not been fully edited and content may change prior to final publication. Citation information: DOI 10.1109/TVT.2026.3661626

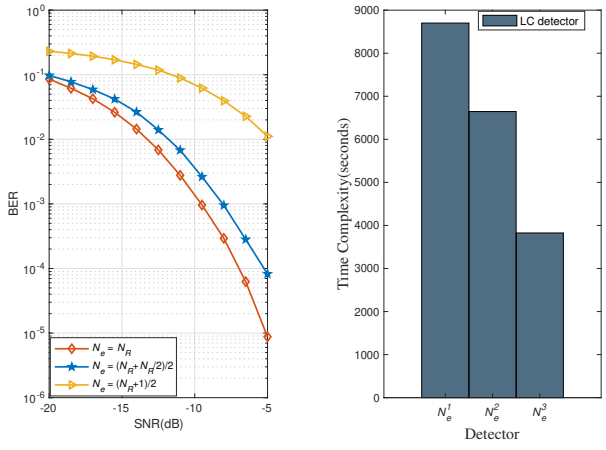

(a) BER performance (b) Time complexity

Fig. 11. The BER performance and complexity of LC detector used in RIS-JTRSSK scheme under different values of N_e.

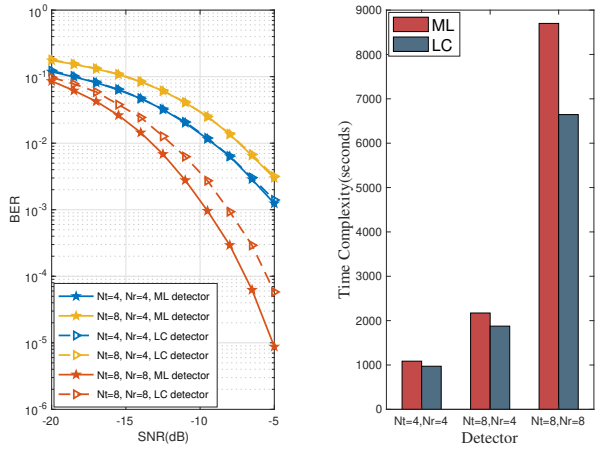

(a) BER performance (b) Time complexity

Fig. 12. The BER performance and complexity of LC detector used in RIS-JTRSSK scheme under N = 64 and $N_e = (N_R + N_R/2)/2$.

AS-JTRSSK and RIS-AS-JTRSSK with FEA exhibit nearly identical performance to RIS-JTRSSK, due to the insufficient number of antenna combinations. When N_T and N_R are increased to 8, compared with RIS-JTRSSK, RIS-AS-JTRSSK can bring 2.5 dB gain to achieve the same BER performance, while the BER performance of RIS-AS-JTRSSK with FEA is moderately worse, due to the influence of the FEA. Furthermore, the FEA demonstrates significant advantages in reducing computational complexity, as shown in Table IV. Specifically, RIS-AS-JTRSSK with FEA reduces the computational load by over 94 percent compared to using MMED alone (RIS-AS-JTRSSK). This indicates that the FEA can substantially lower the computational complexity required by MMED. Therefore, combining the results in Fig. 10 and Table IV, the proposed FEA can achieve much lower complexity and comparable BER performance, which possesses more potential in practical applications.

In Fig. 11, the BER and complexity performance of the different selected numbers N_e are discussed. To illustrate the influence of different N_e, we investigate three most representative values of N_e including: the least one, the middle one and the most one, which can be written as $N_e = (N_R+1)/2$, $N_e = (N_R+\frac{N_R}{2})/2$, and $N_e = N_R$. It can be seen from figure that the increase of N_e improves the BER performance, but the detection complexity also increases. Therefore, considering the BER performance and detection complexity, we choose $N_e = (N_R + \frac{N_R}{2})/2$ as the simulation parameter in the subsequent simulation results, while various N_e values are suitable for different scenarios. And then, the comparisons of BER performance between ML detector and LC detector are investigated in Fig. 12(a), where we set N = 64 and $N_e = (N_R + \frac{N_R}{2})/2$ under different SE cases. As can be seen from the figure, the BER performance of LC detector is close to that of ML detector under the condition of N_T = 4, 8 and N_R = 4, 4, respectively. Besides, in these two cases, the complexity of LC detector is always lower than the one of ML detector, which can be seen in Fig. 12(b). When N_T and N_R are increased to 8, the ML detector provides about 2 dB gain improvement compared with LC detector, but the complexity of ML detector is much higher than that of LC detector. Obviously, LC detector achieves ideally low complexity by sacrificing a portion of BER, especially at high SE. Therefore, LC detector can be regard as the trade-off between BER and complexity, which is efficient in practical applications.

VIII. Conclusion

This paper proposed a generalized RIS-assisted SSK modulation scheme, termed RIS-JTRSSK, for wireless communication systems to enhance SE and provide greater design flexibility. Under perfect CSI assumption, we first established the theoretical superiority of the proposed scheme through engineering-oriented analysis, while also examining the impact of imperfect CSI. A closed-form BER upper bound was derived using ML detection. Furthermore, we introduced RIS-FTRSSK as an alternative scheme to accommodate diverse application scenarios with higher SE requirements. Simulation results demonstrated that both proposed schemes outperform existing RIS-assisted IM schemes in BER performance, with RIS-JTRSSK achieving higher SE using the same number of antennas while maintaining comparable system complexity. To further optimize performance, we developed an MMED-based antenna selection method and introduced two low-complexity solutions: FEA for simplified antenna selection and LC detector for efficient signal detection, both achieving significant complexity reduction without compromising BER performance. In future work, one key direction is to derive the theoretical BER under imperfect CSI models. Meanwhile, the system performance of the proposed scheme under non-fixed SE conditions is another key direction for our future work. In addition, the proposed scheme can be extended to SM technology related model for other application scenarios in the future, such as IoT application, where artificial intelligence techniques can be leveraged to explore antenna selection algorithms.

Authorized licensed use limited to: University of Waterloo. Downloaded on March 25,2026 at 00:16:41 UTC from IEEE Xplore. Restrictions apply.
© 2026 IEEE. All rights reserved, including rights for text and data mining and training of artificial intelligence and similar technologies. Personal use is permitted, but republication/redistribution requires IEEE permission. See https://www.ieee.org/publications/rights/index.html for more information.

This article has been accepted for publication in IEEE Transactions on Vehicular Technology. This is the author's version which has not been fully edited and content may change prior to final publication. Citation information: DOI 10.1109/TVT.2026.3661626

REFERENCES

[1] E. Basar, M. Wen, R. Mesleh, M. Di Renzo, Y. Xiao, and H. Haas, "Index modulation techniques for next-generation wireless networks," *IEEE Access.*, vol. 5, pp. 16 693–16 746, 2017.

[2] T. Mao, Q. Wang, Z. Wang, and S. Chen, "Novel index modulation techniques: A survey," *IEEE Commun. Surveys Tuts.*, vol. 21, no. 1, pp. 315–348, 2019.

[3] R. Y. Mesleh, H. Haas, S. Sinanovic, C. W. Ahn, and S. Yun, "Spatial modulation," *IEEE Trans. Veh. Technol.*, vol. 57, no. 4, pp. 2228–2241, 2008.

[4] J. Jeganathan, A. Ghrayeb, L. Szczecinski, and A. Ceron, "Space shift keying modulation for mimo channels," *IEEE Trans. Wireless Commun.*, vol. 8, no. 7, pp. 3692–3703, 2009.

[5] K. B. Letaief, W. Chen, Y. Shi, J. Zhang, and Y.-J. A. Zhang, "The roadmap to 6g: Ai empowered wireless networks," *IEEE Commun. Mag.*, vol. 57, no. 8, pp. 84–90, 2019.

[6] M. Yue, Y. Peng, R. Ye, F. Al-Hazemi, M. Meraj Mirza, and J. Lee, "Integration of STAR-RIS with index modulation: Novel attraction solutions for IoT applications," *IEEE Internet Things J.*, vol. 12, no. 14, pp. 27 084–27 096, 2025.

[7] Q. Wu and R. Zhang, "Towards smart and reconfigurable environment: Intelligent reflecting surface aided wireless network," *IEEE Commun. Mag.*, vol. 58, no. 1, pp. 106–112, 2020.

[8] Y. Liu, X. Liu, X. Mu, T. Hou, J. Xu, M. Di Renzo, and N. Al-Dhahir, "Reconfigurable intelligent surfaces: Principles and opportunities," *IEEE Commun. Surveys Tuts.*, vol. 23, no. 3, pp. 1546–1577, 2021.

[9] M. Di Renzo, A. Zappone, M. Debbah, M.-S. Alouini, C. Yuen, J. de Rosny, and S. Tretyakov, "Smart radio environments empowered by reconfigurable intelligent surfaces: How it works, state of research, and the road ahead," *IEEE J. Sel. Areas Commun.*, vol. 38, no. 11, pp. 2450–2525, 2020.

[10] R. Ma, Y. Peng, R. Ye, M. Yue, F. Al-Hazemi, and J. Lee, "Active RIS-assisted secure communications against simultaneous jamming and eavesdropping," *IEEE Wireless Commun. Lett.*, vol. 14, no. 3, pp. 686–690, 2025.

[11] Q. Wu and R. Zhang, "Intelligent reflecting surface enhanced wireless network: Joint active and passive beamforming design," in *Proc. IEEE Global Commun. Conf. (GLOBECOM), Abu Dhabi, UAE, Dec.*, 2018, pp. 1–6.

[12] C. Huang, A. Zappone, G. C. Alexandropoulos, M. Debbah, and C. Yuen, "Reconfigurable intelligent surfaces for energy efficiency in wireless communication," *IEEE Trans. Wireless Commun.*, vol. 18, no. 8, pp. 4157–4170, 2019.

[13] E. Basar, "Reconfigurable intelligent surface-based index modulation: A new beyond mimo paradigm for 6g," *IEEE Trans. Commun.*, vol. 68, no. 5, pp. 3187–3196, 2020.

[14] X. Zhu, L. Yuan, Q. Li, L. Jin, X. Nie, C. Pan, and J. Zhang, "RIS-assisted full-duplex space shift keying: System scheme and performance analysis," *IEEE Trans. Green Commun. Netw.*, vol. 7, no. 4, pp. 1981–1995, 2023.

[15] X. Zhu, W. Chen, Q. Wu, W. Fang, C. Huang, and J. Li, "Robust analysis of full-duplex two-way space shift keying with RIS systems," *IEEE Trans. Commun.*, pp. 1–1, 2024.

[16] A. E. Canbilen, E. Basar, and S. S. Ikki, "Reconfigurable intelligent surface-assisted space shift keying," *IEEE Wireless Commun. Lett.*, vol. 9, no. 9, pp. 1495–1499, 2020.

[17] M. Yue, Y. Peng, and J. Lee, "RIS-assisted flexible space shift keying for wireless communication system," *IEEE Wireless Commun. Lett.*, vol. 12, no. 10, pp. 1776–1780, 2023.

[18] Q. Li, M. Wen, S. Wang, G. C. Alexandropoulos, and Y.-C. Wu, "Space shift keying with reconfigurable intelligent surfaces: Phase configuration designs and performance analysis," *IEEE Open J. Commun. Society.*, vol. 2, pp. 322–333, 2021.

[19] C. Zhang, Y. Peng, J. Li, and F. Tong, "An IRS-aided GSSK scheme for wireless communication system," *IEEE Commun. Lett.*, vol. 26, no. 6, pp. 1398–1402, 2022.

[20] M. Yue, Y. Peng, R. Ye, H. Hai, F. Al-Hazemi, and J. Lee, "IRS-assisted extended variable spatial modulation: A high spectral efficiency scheme," *IEEE Wireless Commun. Lett.*, vol. 13, no. 7, pp. 1838–1842, 2024.

[21] X. Zhu, Q. Wu, and W. Chen, "On the performance of RIS-aided spatial modulation for downlink transmission," *IEEE Trans. Wireless Commun.*, vol. 23, no. 11, pp. 16 203–16 217, 2024.

[22] M. Yue, Y. Peng, Q. Jin, and J. Lee, "RIS-assisted flexible receive spatial modulation for wireless communication," *IEEE Wireless Commun. Lett.*, vol. 14, no. 7, pp. 1859–1863, 2025.

[23] A. E. Canbilen, "On the performance of power-sensing RIS-SM: Effects of improper gaussian noise and nakagami-m fading channel," *Digit. Signal Process.*, vol. 147, p. 104432, 2024.

[24] M. H. Dinan, N. S. Perović, and M. F. Flanagan, "RIS-assisted receive quadrature space-shift keying: A new paradigm and performance analysis," *IEEE Trans. Commun.*, vol. 70, no. 10, pp. 6874–6889, 2022.

[25] M. H. Dinan, M. D. Renzo, and M. F. Flanagan, "RIS-assisted receive quadrature spatial modulation with low-complexity greedy detection," *IEEE Trans. Commun.*, vol. 71, no. 11, pp. 6546–6560, 2023.

[26] X. Zhu, L. Yuan, K. J. Kim, Q. Li, and J. Zhang, "Reconfigurable intelligent surface-assisted spatial scattering modulation," *IEEE Commun. Lett.*, vol. 26, no. 1, pp. 192–196, 2022.

[27] W. Yan, X. Yuan, and X. Kuai, "Passive beamforming and information transfer via large intelligent surface," *IEEE Wireless Commun. Lett.*, vol. 9, no. 4, pp. 533–537, 2020.

[28] S. Guo, S. Lv, H. Zhang, J. Ye, and P. Zhang, "Reflecting modulation," *IEEE J. Sel. Areas Commun.*, vol. 38, no. 11, pp. 2548–2561, 2020.

[29] S. Lin, B. Zheng, G. C. Alexandropoulos, M. Wen, M. D. Renzo, and F. Chen, "Reconfigurable intelligent surfaces with reflection pattern modulation: Beamforming design and performance analysis," *IEEE Trans. Wireless Commun.*, vol. 20, no. 2, pp. 741–754, 2021.

[30] Q. Jin, Y. Peng, F. Al-Hazemi, and J. Lee, "A pattern modulation based IRS scheme for space shift keying communication system," *IEEE Commun. Lett.*, vol. 28, no. 6, pp. 1417–1421, 2024.

[31] K. Kuang-Chi Lee and C.-E. Chen, "New RIS-assisted SSK schemes with passive beamforming using channel-dependent ris partitioning," *IEEE Commun. Lett.*, vol. 29, no. 2, pp. 318–322, 2025.

[32] T. Ma, Y. Xiao, X. Lei, P. Yang, X. Lei, and O. A. Dobre, "Large intelligent surface assisted wireless communications with spatial modulation and antenna selection," *IEEE J. Sel. Areas Commun.*, vol. 38, no. 11, pp. 2562–2574, 2020.

[33] X. Jin, X. Li, Z. Wu, and M. Wen, "RIS-aided joint transceiver space shift keying reflection modulation," *IEEE Commun. Lett.*, vol. 27, no. 3, pp. 891–895, 2023.

[34] G. Zhou, C. Pan, H. Ren, K. Wang, and A. Nallanathan, "A framework of robust transmission design for IRS-aided MISO communications with imperfect cascaded channels," *IEEE Trans. Signal Process.*, vol. 68, pp. 5092–5106, 2020.

[35] B. H. Wang, H. T. Hui, and M. S. Leong, "Global and fast receiver antenna selection for MIMO systems," *IEEE Trans. Commun.*, vol. 58, no. 9, pp. 2505–2510, 2010.

[36] K. Ntontin, M. Di Renzo, A. I. Perez-Neira, and C. Verikoukis, "A low-complexity method for antenna selection in spatial modulation systems," *IEEE Commun. Lett.*, vol. 17, no. 12, pp. 2312–2315, 2013.

[37] P. Wang, J. Fang, H. Duan, and H. Li, "Compressed channel estimation for intelligent reflecting surface-assisted millimeter wave systems," *IEEE Signal Process. Lett.*, vol. 27, pp. 905–909, 2020.

[38] Z.-Q. He and X. Yuan, "Cascaded channel estimation for large intelligent metasurface assisted massive mimo," *IEEE Wireless Commun. Lett.*, vol. 9, no. 2, pp. 210–214, 2020.

[39] J. Mirza and B. Ali, "Channel estimation method and phase shift design for reconfigurable intelligent surface assisted mimo networks," *IEEE Trans. Cogn. Commun. Netw.*, vol. 7, no. 2, pp. 441–451, 2021.

[40] X. Wei, D. Shen, and L. Dai, "Channel estimation for RIS assisted wireless communications—part ii: An improved solution based on double-structured sparsity," *IEEE Commun. Lett.*, vol. 25, no. 5, pp. 1403–1407, 2021.

[41] G. Zhou, C. Pan, H. Ren, P. Popovski, and A. L. Swindlehurst, "Channel estimation for RIS-aided multiuser millimeter-wave systems," *IEEE Trans. Signal Process.*, vol. 70, pp. 1478–1492, 2022.

[42] X. Zhu, W. Chen, Q. Wu, Z. Li, J. Li, S. Zhang, and M. Ding, "Reconfigurable-intelligent-surface-aided space-shift keying with imperfect CSI," *IEEE Internet Things J.*, vol. 11, no. 7, pp. 11 480–11 495, 2024.

[43] A. E. Canbilen, E. Basar, and S. S. Ikki, "On the performance of RIS-assisted space shift keying: Ideal and non-ideal transceivers," *IEEE Trans. Commun.*, vol. 70, no. 9, pp. 5799–5810, 2022.

Authorized licensed use limited to: University of Waterloo. Downloaded on March 25,2026 at 00:16:41 UTC from IEEE Xplore. Restrictions apply.
© 2026 IEEE. All rights reserved, including rights for text and data mining and training of artificial intelligence and similar technologies. Personal use is permitted, but republication/redistribution requires IEEE permission. See https://www.ieee.org/publications/rights/index.html for more information.

This article has been accepted for publication in IEEE Transactions on Vehicular Technology. This is the author's version which has not been fully edited and content may change prior to final publication. Citation information: DOI 10.1109/TVT.2026.3661626

Ming Yue received the B.S. in electronic and information engineering and M.S. in communication engineering from Macau University of Science and Technology (MUST), Taipa, Macau in 2021 and 2023, respectively, where he is currently pursuing the Ph.D. degree in electronic information technology. His research interests include spatial modulation, RIS aided communications, antenna selection, and the Internet of Things (IoT).

Yuyang Peng (M'16-SM'20) received the M.S. and Ph.D. degrees in electrical and electronic engineering from Chonbuk National University, Jeonju, Korea in 2011 and 2014, respectively. He worked as a Postdoctoral Research Fellow in Korea Advanced Institute of Science and Technology (KAIST), Daejeon, South Korea, from 2014 to 2018. He is currently an Associate Professor with the School of Computer Science and Engineering at Macau University of Science and Technology (MUST), Taipa, Macau. His research activities lie in the broad area of digital communications, wireless sensor networks, and computing. In particular, his current research interests include cooperative communications, spatial modulation, and communication security. He served as an Editor for IEEE Access.

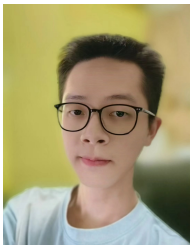

Runlong Ye received the B.E. degree in communication engineering from Zhuhai College of Science and Technology (ZCST), Zhuhai, China, in 2020, and the M.S. degree in communication engineering from Macau University of Science and Technology (MUST), Macau SAR, China, in 2022, where he is currently pursuing the Ph.D. degree in electronic information technology. His research interests include physical layer security, RIS-assisted communications, and integration of sensing and communications.

Juho Lee (Fellow, IEEE) received the B.S., M.S., and Ph.D. degrees in electrical engineering from the Korea Advanced Institute of Science and Technology (KAIST), South Korea, in 1993, 1995, and 2000, respectively. In 2000, he joined Samsung Electronics and he has worked on multiple generations of mobile communications, such as WCDMA and HSDPA in 3G, LTE, LTE-Advanced, and LTE-Advanced Pro in 4G and 5G NR technologies. He is currently a fellow (EVP of technology) with Samsung Electronics, where he is also working on research and standardization for mobile communications. His current research interests include the preparation of future technologies, such as 5G evolution, e.g., 5G-advanced in 3GPP and 6G. He was the Vice Chair of 3GPP RAN WG1 from February 2003 to August 2009 and chaired LTE/LTE-Advanced MIMO sessions. He also served as the rapporteur of the work item for specifying CoMP in 3GPP LTE-Advanced Rel-11. He serves as the Guest Editor for IEEE Communications Standards Magazine.

Fawaz AL-Hazemi (M'04-SM'16) received the B.S. degree in computer engineering from King Fahd University of Petroleum and Minerals (KFUPM), Dhahran, Saudi Arabia, in 2003 and the M.S. and Ph.D. degrees from Korea Advanced Institute of Science and Technology (KAIST), Daejeon, South Korea, in 2010 and 2019, respectively. He is currently working as an Assistant Professor at College of Computer Science and Engineering, University of Jeddah, Saudi Arabia. Also, he is the Deputy supervisor of digital transformation and Information Technology (IT) center in University of Jeddah. His research interests are green data center, energy-aware computing, and communications.

Raouf Boutaba (F'12) received the M.Sc. and Ph.D. degrees in computer science from Sorbonne University in 1990 and 1994, respectively. He is currently a University Chair Professor and the Director of the David R. Cheriton School of Computer science at the University of Waterloo (Canada). His research interests fall in the areas of computer networking and distributed systems. Dr. Boutaba served as the founding Editor-in-Chief of the IEEE Transactions on Network and Service Management (2007-2010) and the Editor-in-Chief of the IEEE Journal on Selected Areas in Communications (2018-2021). He is a fellow of the IEEE, the Engineering Institute of Canada, the Canadian Academy of Engineering, and the Royal Society of Canada.

Authorized licensed use limited to: University of Waterloo. Downloaded on March 25,2026 at 00:16:41 UTC from IEEE Xplore. Restrictions apply.
© 2026 IEEE. All rights reserved, including rights for text and data mining and training of artificial intelligence and similar technologies. Personal use is permitted, but republication/redistribution requires IEEE permission. See https://www.ieee.org/publications/rights/index.html for more information.